Colloids and Surfaces A: Physicochem. Eng. Aspects 506 (2016) 127–137

Contents lists available at ScienceDirect

Colloids and Surfaces A: Physicochemical and Engineering Aspects

journal homepage: www.elsevier.com/locate/colsurfa

A comprehensive numerical investigation of DC dielectrophoretic particle–particle interactions and assembly

Mohammad R. Hossan [a,b,*], Partha P. Gopmandal [c], Robert Dillon [d], Prashanta Dutta [e]

[a] Department of Engineering and Physics, University of Central Oklahoma, OK 73034, United States
[b] Center for Interdisciplinary Biomedical Education and Research (CIBER), University of Central Oklahoma, OK 73034, United States
[c] Department of Mathematics, National Institute of Technology-Patna, Bihar 800005, India
[d] Department of Mathematics, Washington State University, Pullman, WA 99164-3113,United States
[e] School of Mechanical and Materials Engineering, Washington State University, Pullman, WA 99164-2920, United States

HIGHLIGHTS

- Impact of size and shape of particles on dielectrophoretic assembly is presented.
- Dielectrophoretic force on elliptical particles depends on the orientations.
- The interaction time span depends on the particles size as well as shape.
- Electrically similar particles form chain along the direction of electric field.
- Electrically dissimilar particles form chain in orthogonal to the electric field.

GRAPHICAL ABSTRACT

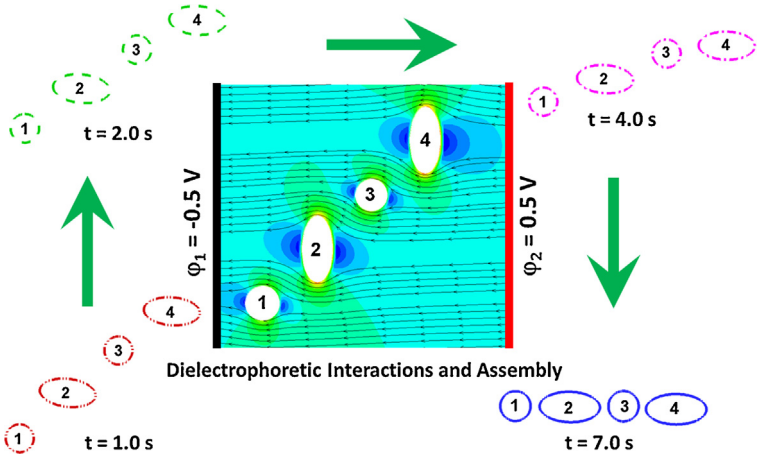

ARTICLE INFO

Article history:
Received 26 March 2016
Received in revised form 10 June 2016
Accepted 16 June 2016
Available online 17 June 2016

Keywords:
Dielectrophoresis
Particle–particle interactions
Particle assembly
Immersed interface method
Immersed boundary method

ABSTRACT

This paper presents a comprehensive numerical study of dielectrophoretic (DEP) interactions and assembly of particles with various size, shape and electrical properties. A hybrid immersed boundary-immersed interface method is employed to solve coupled electric field and fluid flow equations. DEP forces are estimated from Maxwell's stress tensor. Results show that the final orientation depends on the electrical properties of the particles and fluid media. Particles that are identical in their electrical conductivities form an assembly parallel to the applied electric field regardless of their sizes, shapes and initial orientations. On the other hand, particles with dissimilar electrical conductivities (i.e. combination of more and less conductivities than the fluid media) form an assembly perpendicular to the electric field regardless of their sizes, shapes and initial positions. However, the interaction time span depends on the particles size and shape. In parallel assembly, particles rotate in a clockwise direction, while in perpendicular assembly particles rotate in counter-clockwise direction to reach to the final orientation.

* Corresponding author at: Department of Engineering and Physics, University of Central Oklahoma, OK 73034, United States.
E-mail addresses: mhossan@uco.edu, robiulme@gmail.com (M.R. Hossan).

http://dx.doi.org/10.1016/j.colsurfa.2016.06.027

The simulation results qualitatively match with the experimental observation. This study provides critical insight on DEP interactions and assembly for a class of particles.

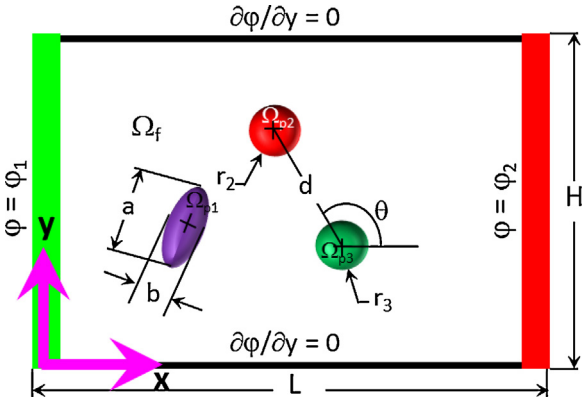

Fig. 1. Schematic representation of a rectangular domain that contains particles (Ω_p) with different sizes and shapes in a fluid medium (Ω_f). The center to center distance, d and initial orientation angle, θ of the particle 2 and particle 3 are shown. The major and minor axis of the elliopsoidal particle are denoted as a and b, respectively. The electric potential is applied on the left (φ_1) and right (φ_2) boundaries while top and bottom boundaries are insulated ($\partial\varphi/\partial y = 0$).

1. Introduction

Recently the study of dielectrophoretic (DEP) particle–particle interactions and assembly has become a subject of growing interest to diverse fields such as colloidal, biological, electronic, photonic, magnetic and biomaterials research [1–3]. In DEP particle manipulation, an electric field either DC, or AC, or a combination of AC and DC is applied. The applied electric field polarizes particles, which causes a net force on the particles due to the effect of the electric field on the polarized electrical charges. The DEP force facilitates particle–particle interaction and assembly formation. DEP force is highly sensitive to the size and shape of particles, electrical properties of particles and fluids, and electric field parameters such as magnitude and frequency [4,5].

DEP interactions and particle assembly have been demonstrated in the development of functional biological structures as well as engineered materials with desired properties [6,7]. For instance, a DEP mechanism was employed to assemble, align and package semiconducting nanotubes, and form electronically functional nanotube arrays for high performance electronic devices [8]. Velev and coworkers reported the formation of electrically functional microwires between planar electrodes [9] and a biocompatible material by patterning live cell and functionalized particles using DEP [10]. Huan et al. [11] used a similar technique to create multilayered cellular structures mimicking bone-like tissue in a 3D scaffold. The creation of an engineered Hematon—a blood producing cellular microenvironment- was also reported in the literature using DEP cell assembly [12].

In support of experimental exploration, an ongoing effort is being made to better understand the underlying mechanism of DEP by developing numerical simulations [13]. In general, numerical simulations involve solution of electric and flow fields with proper estimation of DEP and hydrodynamic forces acting on the constituent particles. Based on the force estimation, there are two approaches for modeling and simulation of DEP [13]. In a simplified approach, effective dipole moment (EDM) and Stokes drag (SD) approximations are used to calculate DEP and hydrodynamic force respectively [13]. Rosenthal and Voldman [14] used this simplified model to simulate and verify experimental observation of DEP cell patterning in a microfluidic trap. A similar approach was used by other researchers as well [15–17]. However, the simplified approach has limited application in microfluidics because these approximations do not hold when particles are close to each other or to boundary walls. Also this type of simplified model is not useful for nonspherical particles or if particle size is comparable with microfluidic dimension [13,18,19].

An interface resolved approach addresses the limitation of the simplified approach [13] by using the Maxwell's stress tensor (MST) and Cauchy stress tensor (CST) to estimate DEP and hydrodynamic forces respectively. Hossan et al. [20–22] developed a hybrid immersed interface-immersed boundary method to study the effect of electrical conductivities and particle size on DEP particle–particle interaction and assembly. Other methods such as arbitrary Lagrangian-Eulerian (ALE) method [23,24], boundary element method (BEM) [25], finite volume based sharp interface method [26] and Lagrange distributed method [27] have also been used to study DEP interaction between spherical shaped particles using stress tensor approach. Recently we extended our hybrid immersed interface-immersed boundary method to study the interactions of elliptical bipolar particles [28]. Note that the aforementioned studies were limited to the investigation of DEP interactions between identical circular or elliptical particles.

Recent experimental studies report that the interactions and assembly of irregularly shaped particles are important for development of smart materials, engineered biological cellular structure and tissue formation [29,30]. The size, shape and electric field parameters has significant impact on DEP interactions and particle assembly [31]. To the best of our knowledge, there have been no comprehensive studies that report the interactions or assembly among particles of different shapes, size and electrical properties. In this paper, we present a systematic comprehensive numerical study of DEP interactions and assembly of both identical and nonidentical particles with respect to their size, shape and electrical properties. The electric field and fluid flow equations are solved using our hybrid immersed interface-immersed boundary method. The results of interaction and assembly of nonidentical particles are compared with the results of corresponding identical particles.

2. Theory

The application of electric field causes accumulation of net electrical charges along the interface between fluid and particles because of polarization. In a spatially nonuniform electric field, particles experience a net force due to the action of the electric field on the accumulated charges. This dielectrophoretic (DEP) force can be used to manipulate particles in fluid media. Both AC and DC electric field can create DEP forces and work equally on charged or neutral particles. In this study, we employ DC electric field to facilitate DEP. However application of DC electric field introduces other electrokinetic effects such as electrophoresis and electroosmosis. Since particles in this study are electrically neutral and of micrometer scale, these effects are ignored. A detailed justification can be found elsewhere [21,23,25].

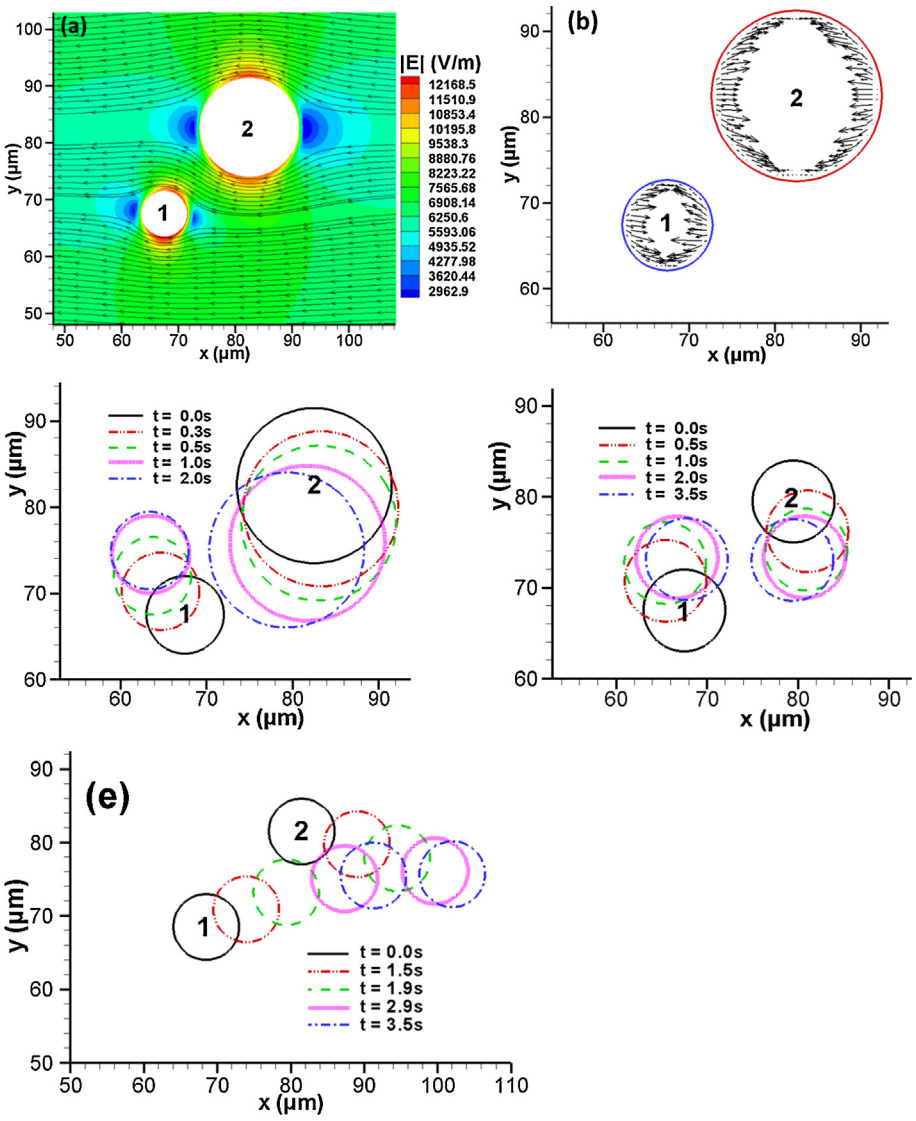

Fig. 2. (a) Electric field distribution at particles' initial position. (b) DEP force distribution on the particles' surface at the initial position. Snapshots of interaction at different times between (c) large (r = 4.5 μm) and small (r = 4.5 μm) particles and (d) two same size small particles of 1×10^{-5} S/m electrical conductivity (e) two same size small particles with electrical conductivity of 1×10^{-3} S/m. Initial orientation between particles is 45° and particles are apart from each other by 8.5 μm.

2.1. Governing equations and boundary conditions

We focus on a system of multiple particles with various sizes and shapes suspended in an incompressible Newtonian viscous fluid as shown in Fig. 1. DEP can be described with two sets of governing equations for electric and flow fields [20]. The electric field distribution for the system is given by the Maxwell's quasi-electrostatic law [32]:

$$\nabla \cdot (\nabla) = 0\tilde{\varepsilon}\tilde{\varphi} \tag{1}$$

where $\tilde{\varphi} = \varphi(\vec{x})e^{j\omega t}$ is the complex electric potential and $\tilde{\varepsilon} = \varepsilon - j\frac{\sigma}{\omega}$ is the complex permittivity. Here, ε is the permittivity, σ is the electrical conductivity and $\omega = 2\pi f$ is the angular frequency; f is the frequency of the applied electric field. For DC DEP, the frequency goes to zero and Eq. (1) simplifies to:

$$\nabla \cdot (\sigma \nabla \varphi) = 0 \tag{2}$$

In order to solve Eq. (2), the following boundary conditions are used:

$$\varphi(0, y) = \varphi_1 \tag{3}$$

$$\varphi(L, y) = \varphi_2 \tag{4}$$

$$\frac{\partial \varphi}{\partial y}\Big|_{y=0} = \frac{\partial \varphi}{\partial y}\Big|_{y=H} = 0 \tag{5}$$

In addition, the continuity of the electric potential and the normal component of the electric flux density are imposed at the interface of each particle as follows:

$$\varphi_p = \varphi_f \tag{6a}$$

$$\sigma_p \frac{\partial \varphi_p}{\partial \vec{n}} = \sigma_f \frac{\partial \varphi_f}{\partial \vec{n}} \tag{6b}$$

where the subscript p refers to the particle and f refers to the fluid at the interface, and $\vec{n}$ is the surface normal. The electric field is given by:

$$\vec{E} = -\nabla \varphi \tag{7}$$

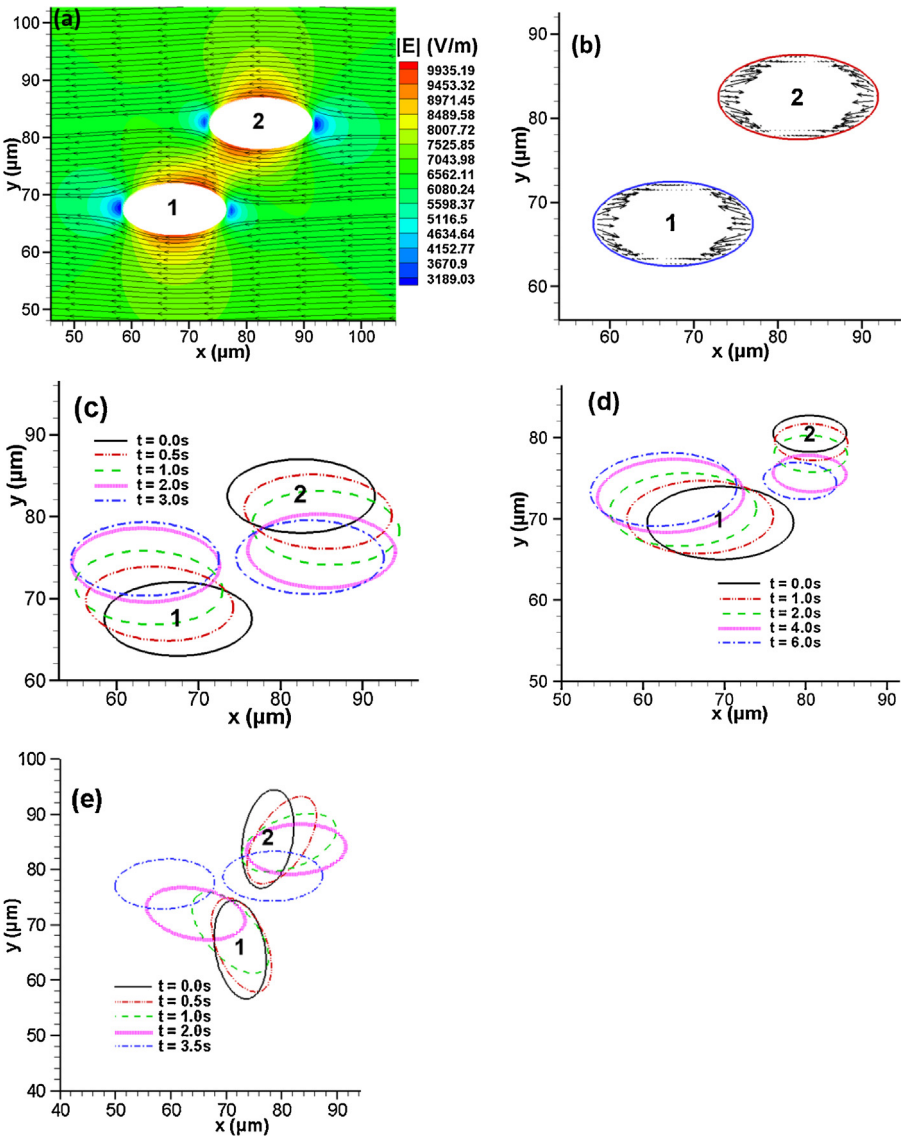

Fig. 3. Interactions between electrically similar elliptical particles. (a) Electric field distribution at particles' initial position. (b) DEP force distribution around the particles at the initial position. Transient interactions between (c) larger particles (a = 18 μm, a/b = 2), (d) larger and smaller (a = 9 μm, a/b = 2) particles of $\sigma = 1 \times 10^{-5}$ S/m and (e) larger particles of $\sigma = 1 \times 10^{-3}$ S/m.

The DEP forces are evaluated from the electric field distribution using Maxwell's stress tensor as follows:

$$\vec{F}_{DEP} = \nabla \cdot \left[\varepsilon - \frac{1}{2}\left(\varepsilon \cdot \vec{E}\right)\right] \vec{E}\vec{E} - \frac{\vec{I}}{\rightharpoonup} \vec{E} \tag{8}$$

where $\vec{E}\vec{E}$ is the dyadic product of the electric field and $\rightharpoonup \vec{I}$ is the identity tensor. The fluid flow is governed by the incompressible Navier-Stokes and continuity equation:

$$\rho\left[\frac{\partial \vec{v}}{\partial t} + \left(\vec{v} \cdot \nabla\right)\right] = -\nabla p + \mu \Delta \vec{v} + \vec{F} \tag{9}$$

$$\nabla \cdot \vec{v} = 0 \tag{10}$$

where ρ is the density, $\vec{v}$ is the velocity, p is the pressure and μ is the viscosity of fluid. The last term in Eq. (9) accounts the presence of particle in the fluid as well as dielectrophoretic force as [20]

$$\vec{F} = \vec{F}_{IB} + \vec{F}_{DEP}. \tag{11}$$

where $\vec{F}_{IB}$ is the elastic force that represents particles in the fluid [33] and $\vec{F}_{DEP}$ is the dielectrophoretic force as provided in the Eq. (8). The elastic force can be obtained as

$$\vec{F}_{IB}(\vec{x}, t) = \int_{\Gamma} \vec{f}_{elastic}(s, t)\delta[\vec{x} - \vec{X}(s, t)]ds. \tag{12}$$

Here $\vec{X}(s, t)$ is a parameterization of particle boundary, s is a spatial postion of particle boundary, $\vec{x} = (x, y)$ is spatial position in fluid domain, $\delta(\vec{x})$ is the two dimensional Dirac delta function used to convert particle information to the fluid domain. The local elastic force $\vec{f}(s, t)$ represents particles which is derived from stretching, bending or tethering of particle boundaries based on the material properties. The following boundary conditions are used to solve fluid equations:

$$\left.\begin{aligned} \vec{v} \cdot &= 0\vec{n} \\ \vec{v} \cdot &= 0\vec{\tau} \end{aligned}\right\} \text{ at } y = 0 \text{ and } y = H \tag{13a}$$

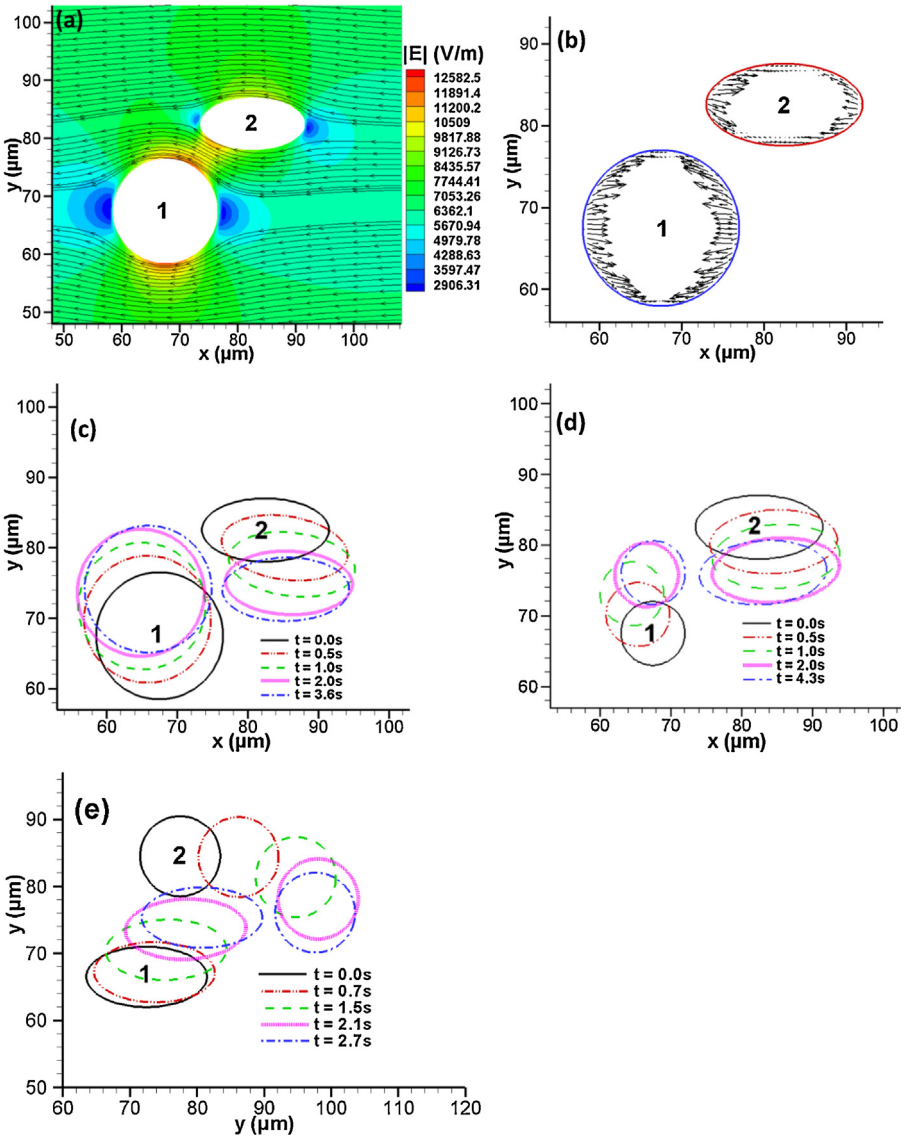

Fig. 4. DEP interaction between electrically similar circular and elliptical shaped particles. At the particles initial position (a) Electric field distribution (b) DEP force distribution. Transient DEP interaction sequences between elliptical (a = 18 μm,a/b = 2) and circular particles of (c) radius, r = 9 μm and (d) radius, r = 4.5 μm with $\sigma = 1 \times 10^{-5}$ S/m and (e) radius, r = 5.0 μm with $\sigma = 1 \times 10^{-3}$ S/m.

$$\left.\begin{aligned} \vec{v}(0,y) &= \vec{v}(L,y) \\ \frac{\partial \vec{v}}{\partial x}\Big|_{x=0} &= \frac{\partial \vec{v}}{\partial x}\Big|_{x=L} \end{aligned}\right\} \text{atx=0 and x=L} \tag{13b}$$

Here, $\vec{\tau}$ is the unit tangent vector. The Eq. (13a) implies no slip and no penetration boundary conditions on the upper and lower boundary of the domain while the Eq. (13b) implies periodic boundary condition on the left and right boundaries of the domain.

3. Numerical methods

The governing equations for fluid flow and electric field are solved by our previously developed hybrid immersed interface-immersed boundary method [20,21,28]. The immersed interface method is efficient and stable especially for elliptic interface problems, while immersed boundary method is robust and accurate for particle-fluid interactions. The details of the numerical method, discretization and formulations, code validation, grid refinement analysis and accuracy of the method can be found in [20,33,34]. Briefly, the electric field Eqs. (2)–(6) are solved by immersed interface method; at any instant of time the solution of electric field Eqs. (2)–(6) are independent of the fluid Eqs. (9)–(11). However, the solution of fluid equations is dependent on the solution of electric field equation through the body force term Eqs. (8)–(11). Therefore both electric field and fluid flow equations are solved sequentially and the position of particles are updated each time step. The fluid Eqs. (9)–(13) are solved by immersed boundary method. A rigorous convergence analysis was performed in our earlier study [20], and it will not be repeated here. Previous convergences study yielded a second order accuracy for immersed interface method, while the numerical accuracy is only first order for the immersed boundary method. The temporal accuracy of the hybrid method is first order. The numerical model was also validated against the experimental result reported in [35] by comparing the levitation of a 6 μm latex particles as a function of applied electric potential though an interdigitized electrode bed.

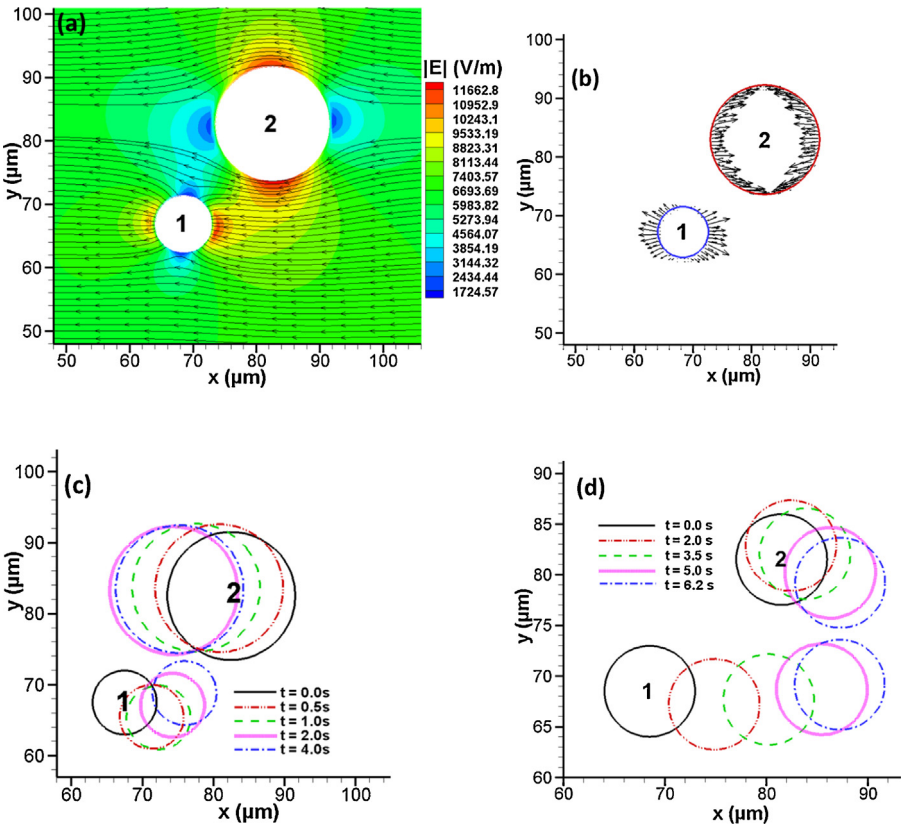

Fig. 5. DEP interactions for electrically dissimilar particles where particle 1 is more conductive and particle 2 is less conductive compared to the fluid media. (a) Electric field distribution (b) DEP force distribution. Snapshots of transient interactions between (c) small and large particles and (d) same sized circular particles.

4. Results and discussion

We studied DEP interactions and assembly of particles with various sizes, shapes, electrical properties, initial positions and orientations in a fluid media. In this section, we present some representative results of this rigorous study. The electrical conductivity of the fluid was kept the same throughout the study and considered as 1×10^{-4} S/m. This conductivity resembles the typical fluid media such as water used in DEP experiments [36]. The electrical conductivities of the particles are varied from case to case. The initial orientation and center to center distance between particles are 45° and 21.25 μm respectively if not mentioned otherwise. The electric potential of −0.5 V and 0.5 V were applied on the left and right boundaries of a 150 μm × 150 μm computational domain. If not mentioned otherwise, the major (a) and minor (b) axes of larger and smaller elliptical particles are 18 μm and 9 μm, and 9 μm and 4.5 μm respectively. The radius (r) of larger and smaller particle is 9 μm and 4.5 μm, respectively.

4.1. Particle-particle interactions: electrically similar particles

This section presents results of DEP interactions between two particles of the same electrical conductivities of 1×10^{-5} S/m or 1×10^{-3} S/m. The following section discusses the result of particle–particle interactions for different shapes, sizes and orientations.

4.1.1. Circular particles

The electric field distribution at the particles' initial position is shown in Fig. 2a for circular particles of different size. Initially particles' surface are 8.5 μm apart from each other. The electric field lines go around the particles because particles are less conductive than the fluid. In other words at the particle surface, the electric field becomes completely tangential and there is no normal component of electric field at the particle surface. Thus a weaker electric field region is created along the direction of applied electric field (right and left of the particles), while a stronger electric field region is created perpendicular to the electric field direction (top and bottom of the particles). The electric field distribution in the domain becomes asymmetric due to the presence of nearby particles. Recall that the asymmetry in the electric field causes DEP on the particles. In the absence of neighbouring particle(s), the electric field would have been symmetric and hence no DEP would have resulted.

The magnitude and direction of the DEP forces varies around the particle surface as shown in Fig. 2b. The force distributions on the adjacent surfaces of the particles are stronger than the other surfaces. This is because the electric field perturbation in the region between the particles is much more pronounced than in the other regions (Fig. 2a). The variation of force distribution on the surfaces contributes to both translational and rotational motion of the particles as seen in Fig. 2c. The direction of the DEP forces are inward to the particle surface i.e. compressive which is the case for negative DEP [21]. It is important to note that the DEP force distribution demonstrates some resolution issue due to the use of lower interpolation scheme. This issue can be resolved by adopting higher order scheme which is computationally expensive. Numerical resolution issues of DEP force distributions are also seen in others cases presented in the following sections.

Fig. 2c depicts the particle locations with time at the various stages of DEP interaction. Particles experience both translational and clockwise rotational motion simultaneously. Smaller particles move faster than larger particles in the earlier time steps, while in later time steps, the larger particles move faster than the smaller particles. For example, at 0.3 s, the smaller particle has traveled

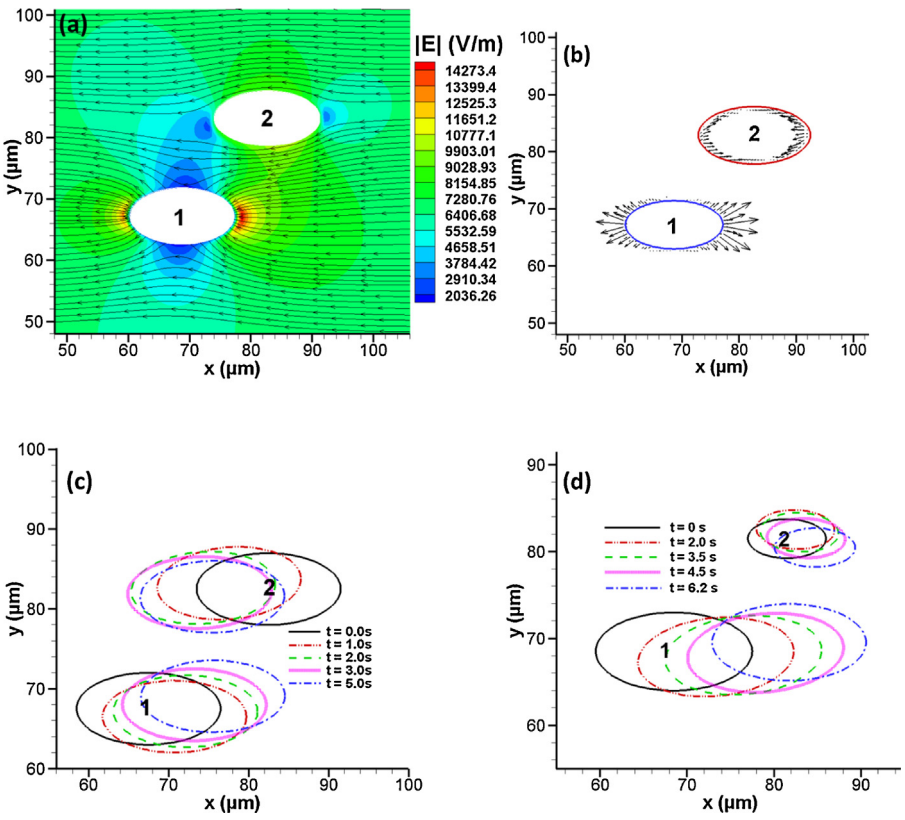

Fig. 6. DEP interactions between electrically dissimilar elliptical particles. The initial orientation and center to center distance are 45° and 21.25 μm respectively. (a) Electric field distribution (b) DEP force distribution. Snapshots of transient interactions between (c) same sized elliptical particles and (d) bigger and smaller elliptical particles.

3.96 μm, whereas the larger particle has traveled 2.76 μm distance. As seen from Fig. 2a, the degree of electric field distortion around the larger particle is more pronounced and attracts smaller particles because of negative DEP. On the other hand, the electric field distortion is weaker around the smaller particle. However, at the later time steps, the perturbation of electric field around the smaller particle becomes stronger because of narrower gap between the particles. The larger particle experiences stronger DEP and moves faster. As the particles approach each other, the retarding hydrodynamic drag force becomes stronger than the DEP force [23]. Thus the motion of particles slows as they approach stable orientation. Fig. 2d shows DEP interaction sequences between two identical (smaller) particles with the same initial orientation (45°) and surface to surface distance (8.5 μm) between particles. Initially particles rotate and re-orient by moving away from each other and later, they attract each other and reach to equilibrium stable orientation. In contrast, the interaction between larger and smaller particles is attractive throughout the process (Fig. 2c). The final orientation for both cases (Fig. 2c and d) are in the direction of electric field although their interaction time span is different. Presence of a larger particle creates higher degree of nonuniformity in the electric field and leads to a stronger DEP force to form an assembly in shorter time span. It is also found that assembly process can be accelerated by increasing the magnitude of electric field (not shown in the figure). Fig. 2e shows the interactions of two smaller particles with electrical conductivity of 1×10^{-3} S/m. This pair of particles act like an conductor because their electrical conductivity is greater than the fluid medium (1×10^{-4} S/m). The interaction dynamics of this pair of particles are different from the case seen in Fig. 2d inspite of having similar initial positions. However in both cases the final orientation is parallel to the applied electric field.

4.1.2. Elliptical particles

Here we consider the interaction of two identical elliptical particles with surface to surface distance of 10.25 μm. The electric field distribution at the initial position is shown in Fig. 3a. Like Fig. 2a, a lower electric field region is created at the left and right sides of the particles while a higher electric field region is created on the top and bottom sides of the particles. As in the previous case, both particles act as an insulator and experience negative DEP. Note that the highest and lowest electric field value around the elliptical particles are much lower than that of the circular particles in Fig. 2a. Fig. 3b shows that the compressive DEP forces are mainly concentrated on the left and right sides of the particles in contrast to the circular particles shown in Fig. 2b. However, if the major axes of the elliptical particles are not aligned with the applied electric field direction, DEP forces are distributed throughout the surface of the particles as shown in later sections.

Fig. 3c shows the particle locations at different times. At the initial stage, the particles move away from each other in the x-direction while moving closer along the y direction. After alignment of their major axes in the direction of electric field, particles attract each other to form assembly. Finally particles reach a stable orientation where the major axis becomes parallel to the electric field. The interactions between larger and smaller elliptical particles are shown in Fig. 3d. Fig. 3e shows the interactions of the two identical (larger) elliptical particles with initial orientation of 80° where both particles are conductive (1×10^{-3} S/m) compared to the fluid medium. In this initial orientation, particles experience electrorotation so that each particle's major axis is parallel to the applied electric field. The elliptical particles attain orientational equilibrium when its field-induced dipole is parallel with the field vector [5]. Particles rotate in clockwise direction and finally reach a stable orientation in the direction of the applied electric field.

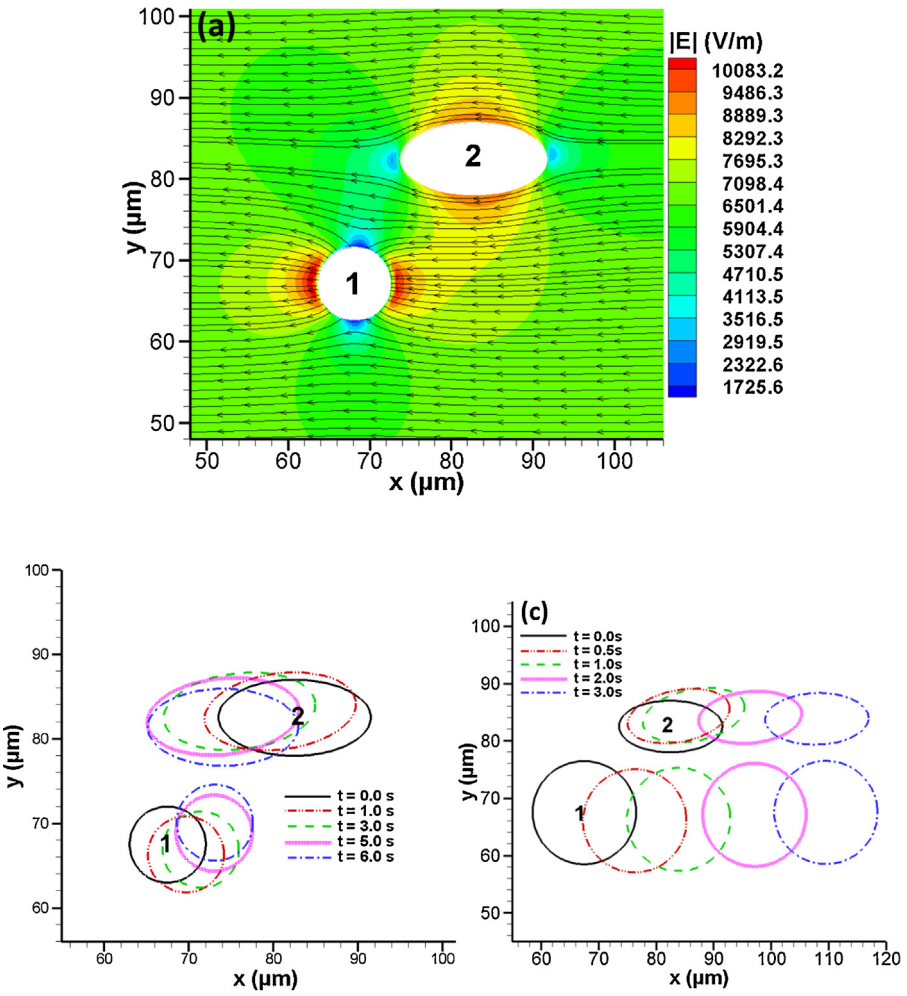

Fig. 7. DEP interactions of dissimilar circular (r = 4.5 μm) and elliptical particles (a/b = 2, b = 9 μm). The initial orientation and center to center distance are 45° and 21.25 μm respectively. (a) Electric field distribution, (b) transient interaction processes of elliptical and smaller circular (r = 4.5 μm particles and (c) transient interaction process of elliptical and larger circular particles (r = 9 μm).

4.1.3. Circular and elliptical particles

We next study a case with an elliptical particle (a = 18 μm, b = 9 μm) and a circular particle (r = 9 μm). The electric field distributions are shown in Fig. 4(a) for the initial orientation of the particles. Our numerical results suggest that the overall electric field distribution and the location of stronger and weaker electric field regions around the particles are similar regardless of their size and shape. DEP force distribution and nature of the forces i.e., compressive or tensile as shown in Fig. 4b are similar to the cases discussed in previous sections. DEP forces on the elliptical particle surface closer to the circular particle is more pronounced due to a higher nonuniformity of electric field in the adjacent region (Fig. 4a). Fig. 4c presents snapshots of particles in the computational domain at various times. The snapshots of particles for a smaller circular particle (4.5 μm radius) with the same elliptical particle are shown in Fig. 4d. In both cases, particles eventually reach a stable final orientation in the direction of the applied electric field. Fig. 4e shows the interaction between a circular particle (r = 5 μm) and a large elliptical particle with initial orientation of 74.5° and center to center distance of 19 μm. Both particles posses electrical conductity of 1×10^{-3} S/m. Final orientation is again in the directin of the electric field. From the results presented in Figs. 2–4, it is clear that the particle size and shape have a strong influence on the time span of particle assembly. Our numerical investigations also reveal that particles still align or form a chain parallel to the applied electric field (not shown in the figure), if the electrical conductivity of both particles is either higher or lower than the fluid conductivity regardless of their individual value. This is because the nature of electric field distribution i.e. local maxima and minima of electric field around the particles remain unaltered.

4.2. Particle-particle interactions: electrically dissimilar particles

Electrically dissimilar particles are particles of different electrical conductivities with respect to the fluid. In this study, we consider two types of particles – one is less conductive (1×10^{-5} S/m) than the fluid medium (1×10^{-4} S/m), while the other type is more conductive (1×10^{-3} S/m) than the fluid medium. The size, initial orientation, interparticle distances are kept same as in the previous sections if not mentioned otherwise.

4.2.1. Circular particles

Here the larger particle is less conductive than the fluid media while the smaller particle is more conductive. The smaller particle acts like a conductor and electric field lines meet the surface at right angles as shown in Fig. 5a. The tangential component of the electric field vanishes at the particle surface by leaving normal component at the surface. This creates locally higher electric field region along the direction of applied electric field and lower electric field region in the perpendicular direction. In contrast, the location of

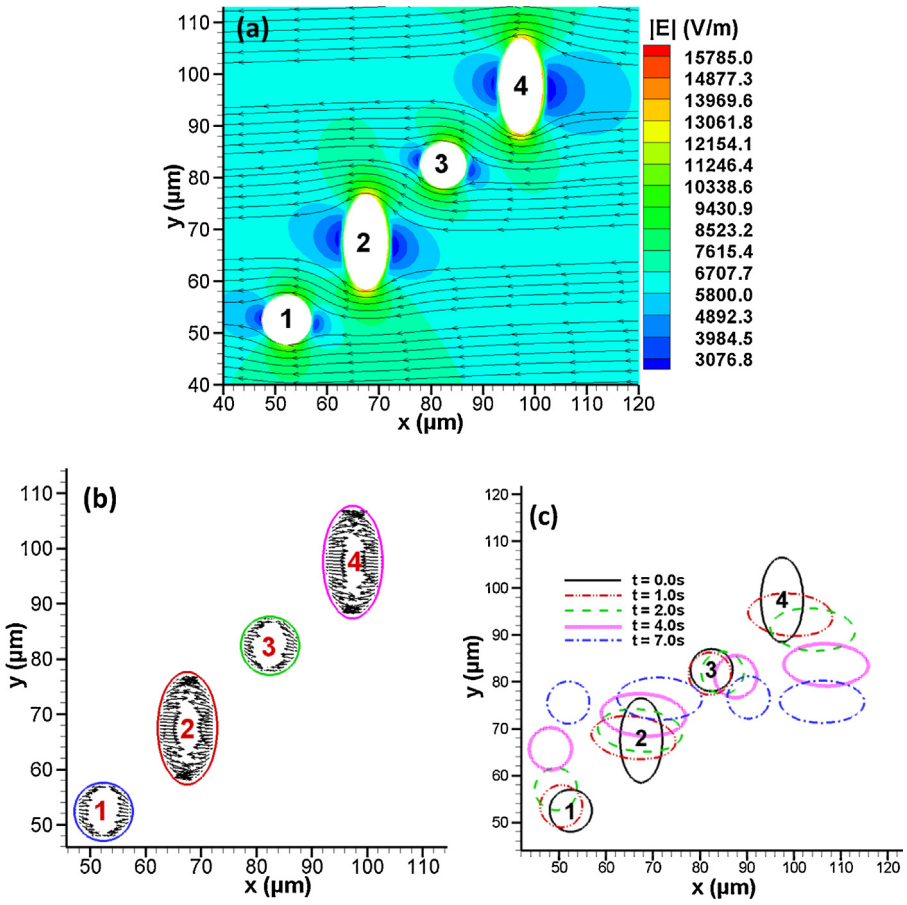

Fig. 8. DEP assembly of similar elliptical and circular particles. The initial orientation and center to center distance between particles are 450 and 21.25 μm, respectively. (a) Electric field distribution, (b) DEP force distribution and (c) transient assembly process.

local higher and lower electric region switch for the larger particle as it is less conductive and hence acts like an insulator. The electric field lines become tangential at the surface of the larger particle with the normal component of electric field becoming zero at the surface.

The DEP force distribution is tensile in nature for smaller particle of greater conductivity while it is compressive for the larger particle with smaller conductivity as in previous cases, as shown in Fig. 5b. Forces on the surfaces adjacent to each other are more pronounced than on distant surfaces. The smaller particle experiences positive DEP and moves toward the locally stronger electric field region (Fig. 5a) which is at the bottom of the larger particle. On the other hand, the larger particle experiences negative DEP and moves towards the locally weaker electric field region which is located at the top of the smaller particle (Fig. 5a). Thus particles approach a final stable orientation in the vertical direction as shown in Fig. 5c. Initially smaller particles moves faster because the degree of nonuniformity of electric field around the larger particle is much higher. However at later time steps, when the smaller particle moves closer to the larger particle, the speed of the larger particle increases due to the increase in electric field gradient. Later the motion of the both particles decelerates. At time t = 4 s, the orientation of the particles is offset by an angle of 2.75° to the transverse direction of the electric field lines. At time t = 5 s, the offset angle decreases to 1.95° (not shown). This angular alignment process is much slower at the subsequent time steps. However, eventually the interacting dissimilar particles align with a perpendicular orientation to the electric field [21]. The DEP interaction for same size (r = 4.5 μm) particles takes longer time to reach final orientation as shown in Fig. 5d because of weaker DEP forces.

4.2.2. Elliptical particles

The electric field distribution is shown in Fig. 6(a) for two same sized elliptical particles at their initial orientation. From the electric field distribution (Fig. 6a), it is evident that the particle 1 is conductive in nature and particle 2 acts like an insulator. The degree of asymmetry in the electric filed is greater in the region between the particles compared to previous cases. The DEP force distributions on the particles surfaces are shown in Fig. 6b. The forces on the particle 1 are tensile while the forces in particle 2 are compressive. Force distribution indicates that the forces on the right sides of the particles are stronger than on the left side of the particles. In other words, the net force on particle 1 is inclined in the positive x-direction while the net force on particle 2 is inclined in the negative x-direction. Thus particle 1 moves toward the positive x-direction and particle 2 moves toward the negative x-direction as shown in Fig. 6c. The particle 2 moves towards the top of the particle 1 for lower electric field region due to negative DEP. On the other hand, particle 1 experiences positive DEP and moves towards the bottom of the particle 2 for higher electric field region. During the interaction processes, the elliptical particles adjust their orientation and move simultaneously closer to each other. However in the circular particle case, particles first orient in the vertical direction and later move toward each other (Fig. 5d). The final orientation for interaction between larger and smaller dissimilar particles is also in the vertical direction i.e. perpendicular to the electric field (Fig. 6d).

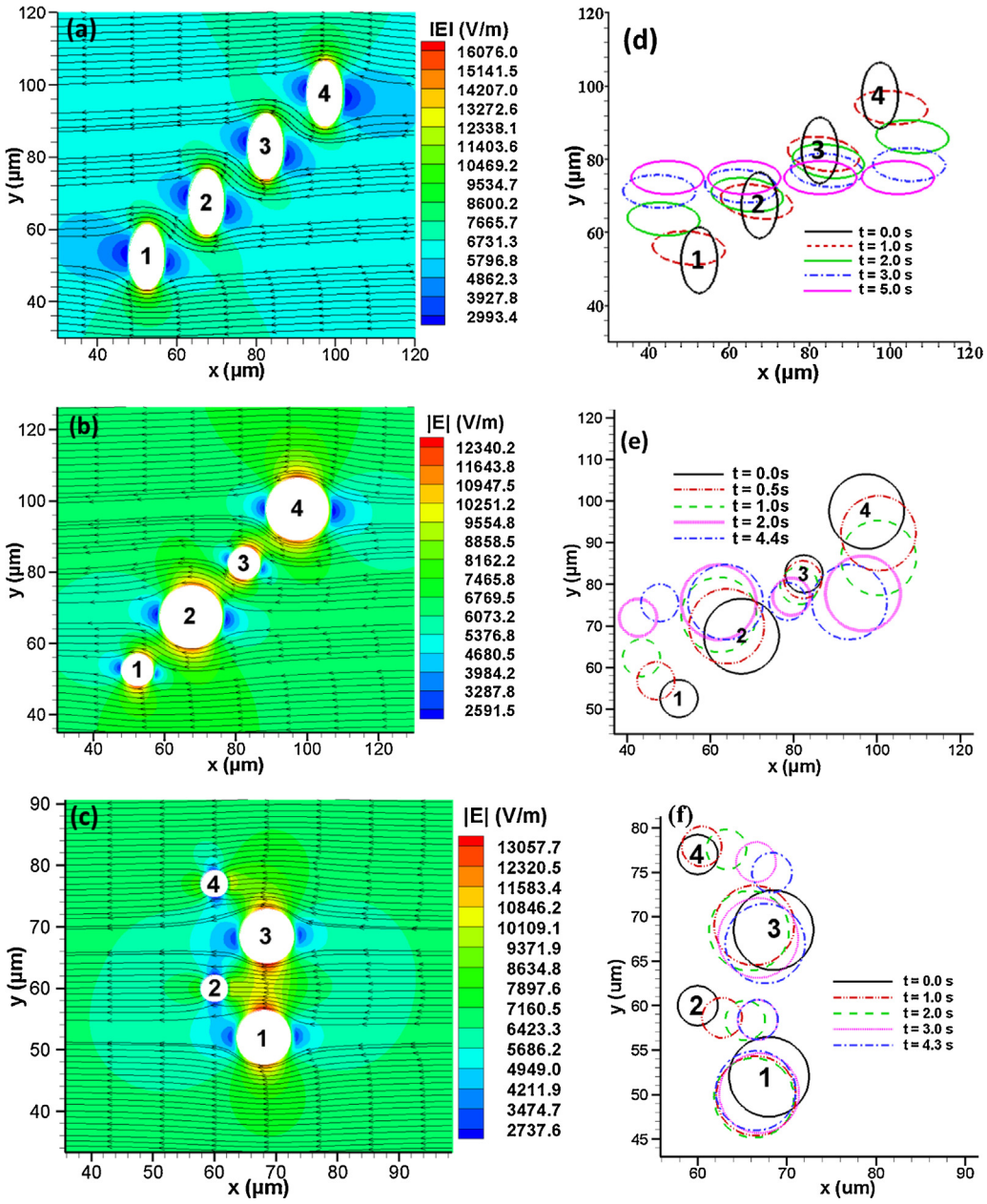

Fig. 9. Electric field distribution of electrically similar (a) elliptical particles, (b) circular particles and (c) electrically dissimilar particles. Transient assembly process of electrically similar (d) elliptical particles, (e) circular particles and (f) electrically dissimilar particles.

4.2.3. Circular and elliptical particles

The DEP interactions between electrically dissimilar elliptical and circular particles are presented in this section. The electric field distribution at the initial position of a circular ($r = 4.5\,\mu m$) and elliptical particle ($a/b = 2$, where $b = 9\,\mu m$) is shown in Fig. 7a. The electric field and DEP distribution (not shown) resembles the dissimilar particle's distribution as seen in previous sections. The transient motion of both particles is shown in Fig. 7b. Both particles experience adjustment in orientation and move closer to each other concurrently to the equilibrium vertical orientation. Fig. 7c depicts the transient interaction processes for larger circular particles with the same initial positions as shown in Fig. 7a. In this case, the distance between the particle surfaces is smaller since the radius of the circular particle was doubled. Particles reach their desired final orientation by lateral movement without much adjustment in orientation.

4.3. Assembly of particles

The DEP particle assembly of various sizes, shapes and electrical properties are presented in this section. The initial electric field distribution is shown in Fig. 8a for two circular and two elliptical particles. Presence of more particles in the domain creates more perturbation in the electric field for the same applied potentials. Because of the greater nonuniformity in electric field distribution, the DEP forces (Fig. 8b) are much stronger than that of the two particles cases (e.g. Fig. 3b). Note that for vertical configuration of elliptical particles (i.e. major axis is perpendicular to the applied electric field) the DEP forces are distributed throughout the particle surface (Fig. 8b), while DEP forces on the elliptical particle in horizontal orientation (i.e. major axis is parallel to the applied electric field) are mainly concentrated on the two sides of the particles (Fig. 3b). Fig. 8c shows that the elliptical particles along with the neighbouring circular particles experiences a clockwise rota-

tion at earlier time steps and align the major axes with the applied electric field. As time goes on, the particles first move away from each other in such a way that the line joining their centers becomes parallel to the electric field direction. The elliptical particle attains orientational stability when its field induced dipole is parallel to the electric field vector [5]. Finally they form an assembly parallel to the electric field.

The assembly of elliptical and circular particles of different sizes and electrical properties are presented in Fig. 9. The electric field distribution of electrically similar elliptical and circular particles are shown in Fig. 9a and b respectively. The nature of electric field distribution, DEP force distribution (not shown) and assembly processes (Fig. 9d and e) resemble the regular negative DEP driven interactions between particles as shown in the Section 4.1. The assembly formation of electrically dissimilar circular particles with different sizes ($r = 4.5\ \mu m$ and $r = 2.25\ \mu m$) are shown in Fig. 9c and f. The electric field and DEP force distribution, and assembly processes are similar to the cases presented in Section 4.2. Note that the particles at the extreme ends move longer distances to form a chain in all cases. This is because only one side of the end particles takes part in interaction, while for middle particles both sides take part in the interaction process.

5. Conclusions

This research presents a comprehensive, systematic study of DEP particle–particle interactions and assembly of various sizes, shapes, initial positions and orientations, and electrical properties. A hybrid immersed boundary-immersed interface method is employed to solve coupled electric field and fluid flow equations. The electric field was solved using the immersed interface method, while the flow field was solved by the immersed boundary method. The DEP forces are calculated from Maxwell's stress tensor (MST). Based on the numerous numerical tests and analysis, the following conclusions are made:

- Presence of particles within a close proximity can create local asymmetry in electric field which is strong enough for particle–particle interaction and assembly in a uniformly applied electric field.
- Electric field distribution around the particles are not only dependent on the electrical properties of particle and fluid media but also size, shape and orientation of the particles.
- In case of interactions in different sized particles, smaller particles moves faster than larger particles.
- The elliptical particles require longer times to reach final stable orientations compared to circular particles. Depending on the initial orientation, elliptical particles undergo an electro-orientation phase to reach an orientational equilibrium in the earlier phase of interaction.
- In case of negative DEP, particles move in a clockwise direction while in positive DEP particles move in a counter-clockwise direction.
- Electrically similar (dissimilar) particles form a stable assembly along the (perpendicular to the) direction of external electric field regardless of size, shape, initial position and orientation.

Acknowledgments

The supports from the US National Science Foundation (Grant No. 1429702 and DMS 1317671) and UCO computing cluster BUDDY are greatly acknowledged.

References

[1] Y. Xia, B. Gates, Y. Yin, Y. Lu, Adv. Mater. 12 (2000) 693–713.
[2] M. Mastrangeli, S. Abbasi, C. Varel, C. Van Hoof, J.-P. Celis, K.F. Böhringer, J. Micromech. Microeng. 19 (2009) 083001.
[3] M. Li, W. Li, J. Zhang, G. Alici, W. Wen, J. Phys. D: Appl. Phys. 47 (2014) 063001.
[4] H. Morgan, N.G. Green, AC Electrokinetics: Colloids and Nanoparticles, Research Studies Press, 2003.
[5] T.B. Jones, T.B. Jones, Electromechanics of Particles, Cambridge University Press, 2005.
[6] B. Bharti, O.D. Velev, Langmuir 31 (29) (2015) 7897–7908.
[7] M. Grzelczak, J. Vermant, E.M. Furst, L.M. Liz-Marzán, ACS Nano 4 (2010) 3591–3605.
[8] Q. Cao, S.-j. Han, G.S. Tulevski, Nat. Commun. 5 (2014).
[9] K.D. Hermanson, S.O. Lumsdon, J.P. Williams, E.W. Kaler, O.D. Velev, Science 294 (2001) 1082–1086.
[10] S. Gupta, R.G. Alargova, P.K. Kilpatrick, O.D. Velev, Soft Matter 4 (2008) 726–730.
[11] Z. Huan, H.K. Chu, J. Yang, D. Sun, 3D cell manipulation with honeycomb-patterned scaffold for regeneration of bone-like tissues, information and automation, IEEE International Conference On, IEEE (2015) 1680–1685.
[12] G.H. Markx, L. Carney, M. Littlefair, A. Sebastian, A.-M. Buckle, Biomed. Microdevices 11 (2009) 143–150.
[13] T.Z. Jubery, S.K. Srivastava, P. Dutta, Electrophoresis 35 (2014) 691–713.
[14] A. Rosenthal, J. Voldman, Biophys. J. 88 (2005) 2193–2205.
[15] K.H. Kang, D. Li, Langmuir 22 (2006) 1602–1608.
[16] N. Aubry, P. Singh, EPL (Europhys. Lett.) 74 (2006) 623.
[17] P. Singh, N. Aubry, Phys. Rev. E 72 (2005) 016602.
[18] M. Robiul Hossan, R. Dillon, P. Dutta, J. Comput. Phys. 270 (1) (2014) 640–659.
[19] Y. Liu, W.K. Liu, T. Belytschko, N. Patankar, A.C. To, A. Kopacz, J.H. Chung, Int. J. Numer. Methods Eng. 71 (2007) 379–405.
[20] M.R. Hossan, R. Dillon, P. Dutta, J. Comput. Phys. 270 (2014) 640–659.
[21] M.R. Hossan, R. Dillon, A.K. Roy, P. Dutta, J. Colloid Interface Sci. 394 (2013) 619–629.
[22] M.R. Hossan, P. Dutta, R. Dillon, Numerical investigation of DC dielectrophoretic particle transport, ASME 2014 4th Joint US-European Fluids Engineering Division Summer Meeting Collocated with the ASME 2014 12th International Conference on Nanochannels, Microchannels, and Minichannels, American Society of Mechanical Engineers (2014) (V002T019A004-V002T019A004).
[23] Y. Ai, S. Qian, J. Colloid Interface Sci. 346 (2010) 448–454.
[24] Y. Ai, Z. Zeng, S. Qian, J. Colloid Interface Sci. 417 (2014) 72–79.
[25] D.L. House, H. Luo, S. Chang, J. Colloid Interface Sci. 374 (2012) 141–149.
[26] S. Kang, Eur. J. Mech.-B/Fluids 54 (2015) 53–68.
[27] J.P. Singh, P.P. Lele, F. Nettesheim, N.J. Wagner, E.M. Furst, Phys. Rev. E 79 (2009) 050401.
[28] M.R. Hossan, P.P. Gopmandal, R. Dillon, P. Dutta, Electrophoresis 36 (5) (2015) 722–730.
[29] J. Zhang, E. Luijten, S. Granick, Annu. Rev. Phys. Chem. 66 (2015) 581–600.
[30] M. Lash, M. Fedorchak, J. McCarthy, S. Little, Soft matter 11 (2015) 5597–5609.
[31] C.W. Shields IV, S. Zhu, Y. Yang, B. Bharti, J. Liu, B.B. Yellen, O.D. Velev, G.P. López, Soft Matter 9 (2013) 9219–9229.
[32] Y. Liu, W.K. Liu, T. Belytschko, N. Patankar, A.C. To, A. Kopacz, J.H. Chung, Int. J. Numer. Methods Eng. 71 (2007) 379–405.
[33] C.S. Peskin, J. Comput. Phys. 25 (1977) 220–252.
[34] Z. Li, SIAM J. Numer. Anal. 35 (1998) 230–254.
[35] G.H. Markx, R. Pethig, J. Rousselet, J. Phys. D: Appl. Phys. 30 (1997) 2470.
[36] T.B. Jones, M. Gunji, M. Washizu, M. Feldman, J. Appl. Phys. 89 (2001) 1441–1448.